



Elevated Atmospheric CO₂ Modifies Mostly the Metabolic Active Rhizosphere Soil Microbiome in the Giessen FACE Experiment

David Rosado-Porto^{1,2} · Stefan Ratering¹ · Massimiliano Cardinale³ · Corinna Maisinger¹ · Gerald Moser⁴ · Marianna Deppe⁴ · Christoph Müller^{4,5} · Sylvia Schnell¹

Received: 19 March 2021 / Accepted: 8 June 2021 / Published online: 19 June 2021
© The Author(s) 2021

Abstract

Elevated levels of atmospheric CO₂ lead to the increase of plant photosynthetic rates, carbon inputs into soil and root exudation. In this work, the effects of rising atmospheric CO₂ levels on the metabolic active soil microbiome have been investigated at the Giessen free-air CO₂ enrichment (Gi-FACE) experiment on a permanent grassland site near Giessen, Germany. The aim was to assess the effects of increased C supply into the soil, due to elevated CO₂, on the active soil microbiome composition. RNA extraction and 16S rRNA (cDNA) metabarcoding sequencing were performed from bulk and rhizosphere soils, and the obtained data were processed for a compositional data analysis calculating diversity indices and differential abundance analyses. The structure of the metabolic active microbiome in the rhizospheric soil showed a clear separation between elevated and ambient CO₂ ($p=0.002$); increased atmospheric CO₂ concentration exerted a significant influence on the microbiomes differentiation ($p=0.01$). In contrast, elevated CO₂ had no major influence on the structure of the bulk soil microbiome ($p=0.097$). Differential abundance results demonstrated that 42 bacterial genera were stimulated under elevated CO₂. The RNA-based metabarcoding approach used in this research showed that the ongoing atmospheric CO₂ increase of climate change will significantly shift the microbiome structure in the rhizosphere.

Keywords RNA metabarcoding · Elevated CO₂ · Rhizosphere microbiome · Grassland

Introduction

The rise of atmospheric carbon dioxide (CO₂) concentrations and global warming are well-documented processes. Total annual anthropogenic greenhouse gas emissions have continued to increase, comprising CO₂, which represents

around 75% of these emissions [1]. Elevated CO₂ (eCO₂) concentrations have several consequences on plants, such as increased growth in C3, C4, and CAM plants by 41%, 22%, and 15%, respectively [2, 3]; increased plant yield [4]; decreased evapotranspiration of both C3 [5] and C4 plants [6]; augmented photosynthetic capacity [3, 7, 8]; and increased below-ground biomass [9].

Considering that nearly up to 21% of all photosynthetically fixed carbon is transferred to the rhizosphere, roots and root exudates influence the composition and biomass of soil microbiome [10, 11]. Elevated atmospheric CO₂ increases efflux amounts of total soluble sugars, amino acids, phenolic acids, and organic acids in the root exudates [12–14]. Similarly, the rates of organic carbon as energy sources enhance microbial degradation of soil organic matter (SOC), also known as priming effect [14]. Priming effect is defined as an accelerated decomposition of SOC due to an increased supply of labile C to the soil and changes in the microbial activity as a response [15]. The microbial succession is accompanied by the activation of various, previously

✉ Sylvia Schnell
Sylvia.Schnell@umwelt.uni-giessen.de

¹ Institute of Applied Microbiology, Justus Liebig University, Giessen, DE, Germany

² Faculty of Basic and Biomedical Sciences, Simón Bolívar University, Barranquilla, Colombia

³ Department of Biological and Environmental Sciences and Technologies, University of Salento, Via Prov.le Monteroni, 73100 Lecce, Italy

⁴ Institute of Plant Ecology, Justus Liebig University, Giessen, DE, Germany

⁵ School of Biology and Environmental Science and Earth Institute, University College Dublin, Belfield, Dublin, Ireland

dormant microorganisms that respond specifically to the added substrate [15, 16].

The effects of $e\text{CO}_2$ levels on soil ecosystems have been studied in free-air CO_2 enrichment (FACE) experiments, revealing significant effects of rising CO_2 on soil organisms. However, with regard to microbial composition and function related to carbon and nitrogen cycling, mixed results have been obtained. At the BioCON field experiment, it was found that the structure of microbial communities was different between ambient CO_2 ($a\text{CO}_2$) and $e\text{CO}_2$ [17]. Likewise, the abundance of genes involved in labile C degradation and C and N fixation, as RuBisCo, carbon monoxide dehydrogenase (CODH), propionyl-CoA/acetyl-CoA carboxylase (PCC/ACC), *nifH* and *nirS* genes were significantly increased under $e\text{CO}_2$ [18]. Similarly, He et al. [19] and Xiong et al. [20] have reported a shift of soil microbial communities under $e\text{CO}_2$ in a soybean and a maize agro-ecosystem, respectively. These changes included stimulation of key functional genes involved in carbon fixation and degradation, nitrogen fixation, denitrification, methane metabolism, and phosphorus cycling.

Oppositely, some FACE experiments have shown no effects of $e\text{CO}_2$ on soil microbiome structure and activity, as Marhan et al. [21] who described that abundances of both total 16S rRNA genes and nitrate-reducing bacteria were not influenced by CO_2 but by sampling date and depth. Dunbar et al. [22] described that neither bacterial nor fungal community structure nor composition were altered under $e\text{CO}_2$. Pujol Pereira et al. [23] did not find any significant effects of $e\text{CO}_2$ on bacterial abundance, soil C, and N concentrations. Butterly et al. [24] reported that changes in microbial community structure were not detected, although $e\text{CO}_2$ reduced the abundance of C and N functional genes.

The Giessen free-air CO_2 enrichment (Gi-FACE) experiment in Giessen, Germany, has been running since 1998. It is becoming a good predictor model to assess the effects of long-term increased CO_2 concentrations on soil microbiome structure and function. Some studies carried out in this facility aimed to assess these changes. Regan et al. [25] reported that in the Gi-FACE extractable organic carbon, dissolved organic nitrogen, NH_4^+ , NO_3^- , and abundances of genes involved in ammonia oxidation and denitrification depended more on soil depth and moisture gradient than on $e\text{CO}_2$. Similarly, also de Menezes et al. [26] described that increases in atmospheric CO_2 may cause only minor changes in Gi-FACE's soil bacterial community composition and that functional responses of the soil community are due to factors like soil moisture rather than CO_2 concentration. Brenzinger et al. [27] reported that the abundance and composition of microbial communities in the topsoil under $e\text{CO}_2$ presented only small differences from soil under $a\text{CO}_2$

($a\text{CO}_2$), concluding that +20% CO_2 had little to no effect on the overall microbial community involved in N-cycling in the Gi-FACE soil. More recently, Bei et al. [28] described that $e\text{CO}_2$ had significant effects on the functional expression associated to both rhizosphere microbiomes and plant roots; and that abundances of Eukarya relative to Bacteria were significantly decreased in $e\text{CO}_2$ as well.

The question of why some studies reported differences between $e\text{CO}_2$ and $a\text{CO}_2$ while some others did not is still open. Several abiotic and biotic factors could be the reason for the contradictory observations in the different experimental setups described above. However, all such previous studies conducted in the Gi-FACE used a DNA-based metagenomic approach, with the exception of Bei et al. [28], who utilized a metatranscriptomic approach. The disadvantage of using DNA is that, after a cell dies, amplifiable extracellular DNA can remain in soils for weeks to years and may bias DNA-based estimates of the diversity and structure of soil microbial communities [29, 30]. Moreover, Carini et al. [31] reported that DNA from dead cells or free DNA represented a large fraction of microbial DNA in many soils, comprising approximately 40.7% and 40.5% of amplifiable prokaryotic 16S rRNA genes and fungal ITS amplicons, respectively. Therefore, DNA-depending studies may overestimate the richness of the soil microbiome by up to 55% for prokaryotes and 52% for fungi [31] and in consequence may hide the active microorganisms that are involved in soil microbial processes.

A better approach for assessing differences between $e\text{CO}_2$ and $a\text{CO}_2$ is the use of RNA instead of DNA for 16S rRNA metabarcoding analysis. The ribosome numbers are correlated to the metabolic activity of bacteria [32], and different studies showed that, with this approach, the active organisms instead of the dormant ones were assessed [33–35]. Additionally, results of the metatranscriptomic methodological approach on the Gi-FACE soil microbiome reported by Bei et al. [28] demonstrated that RNA instead of DNA is a better predictor of microbiome composition and activity. For this reason, the aims of the present work were (i) to evaluate the effect of long-term $e\text{CO}_2$ concentrations and increased C supply on active soil microbiome through an rRNA-based metabarcoding approach; (ii) to assess the differences between $e\text{CO}_2$ and $a\text{CO}_2$ conditions in rhizosphere and bulk soils; and (iii) to link these differences with environmental factors.

The following questions have been addressed:

1. Is the community structure of active bacteria different between ambient and elevated CO_2 in rhizosphere and/or bulk soil?
2. Which other environmental parameters beside CO_2 shape the community?

Material and Methods

Study Site Description

The Gi-FACE study is located at 50° 32' N and 8° 41.3' E near Giessen, Germany, at an elevation of 172 m above sea level. It consists of three pairs of rings with a diameter of 8 m; each pair consists of an ambient and an elevated CO₂ treatment ring [36]. Since May 1998 until present, elevated CO₂ rings have been continuously enriched by 20% above ambient CO₂ concentrations during daylight hours. Ambient and elevated CO₂ rings are separated by at least 20 m, and each pair is placed at the vertices of an equilateral triangle. The presence of a slight slope within the experimental site (between 0.5 and 3.5°) places the rings on a moisture gradient, such that pair 1 has the lowest mean moisture content (38.8% ± 10.2%) and pair 2 has the highest mean moisture content (46.1% ± 13.2%), whereas pair 3 is intermediate (40.7% ± 11%) [26, 36]. The average annual air temperature and precipitation are 9.4 °C and 580 mm, respectively.

The vegetation is an *Arrhenatheretum elatioris* Br.Bl. *Filipendula ulmaria* subcommunity, dominated by *Arrhenatherum elatius*, *Galium album*, and *Geranium pratense*. At least 12 grass species, 15 non-leguminous herbs and up to 5 legumes with small biomass contributions (<5%) are present within a single plot [37]. The experimental field has not been ploughed for more than 100 years. It has received N fertilization in form of granular mineral calcium ammonium nitrate (40 kg N ha⁻¹ year⁻¹) once a year since 1995 and has been mown twice a year since 1993. The soil at the Gi-FACE site is classified as Fluvisol; its texture is a sandy clay loam over a clay layer, with pH=6.2 and average C and N contents of 4.5% and 0.45%, respectively, as measured in 2001 [36].

Soil Sampling and Physico-chemical Parameter Measurements

Soil sampling was performed utilizing sawed off 50 ml syringes (11 × 3 cm), and four samples were taken to a depth of ~10 cm within each ring in September 2015. Soil cores were gently shaken by hand to remove loosely attached soil (bulk soil), while the soil that remained attached to the roots was considered as rhizosphere soil. Bulk and rhizosphere soils were sieved (<2 mm) and stored at -80 °C for further analyses. Samples from each soil core were classified in four groups considering the CO₂ conditions (ambient and elevated) and the soil habitat (bulk soil and rhizosphere soil).

Ammonium and nitrate concentrations were measured according to Kandeler et al. [38] and Bak et al. [39]. Water

content, dry matter, and water holding capacity of soil samples were measured gravimetrically [40]. Carbon and nitrogen content of soil were measured by pyrolysis coupled to gas chromatography on a EA 1100 elemental analyzer (ThermoQuest, Milan, Italy) using a TCD detector by the Dumas method according to HBU (1996) [41] and VDLUFA (2012) method [42]. Injected CO₂ and CO₂ soil fluxes were determined from August to September 2015. Injected CO₂ was measured at 60 cm above ground with an infrared gas analyzer (LI-COR 6252) [36]. CO₂ soil fluxes were measured weekly using an automated closed dynamic chamber system (LI-COR 8100, LI-COR Inc., Lincoln, Nebraska, USA). Per ring, 4 PVC soil collars (20.3 cm diameter) were permanently installed as chamber bases in 2006 and held vegetation free since 2008. Fluxes were calculated from the increase in CO₂ concentration in the chamber over the 1–3 min closure time as described by Keidel et al. [43].

Central tendency and dispersion measures were calculated for soil chemical data. CO₂ injection and CO₂ fluxes data were analyzed using growth curve analysis (GCA) [44], with R packages *gazer* version 0.1 [45] and *lme4* version 1.1–23 [46], creating polynomial-transformed predictor variables, fitting them to a linear mixed model by maximum likelihood, and assessing differences between CO₂ conditions with a t-test, using an alpha of <0.05.

RNA Extraction and Reverse Transcription

RNA extraction was performed following a modified protocol of Mettel et al. [47]. For the extraction, 0.3–0.5 g of soil were weighed in reaction tubes containing 100 mg of sterile zirconia beads, added with 700 µl TPM buffer (50 mM Tris-HCl (pH 5), 1.7% [wt/vol] polyvinylpyrrolidone, 20 mM MgCl₂), and vortexed for 30 s. Cells were then disrupted in a cell mill MM200 (Retsch, Haan, Germany) for 2 min at a frequency of 30 Hz. Soil and cell debris were precipitated by centrifugation in a microcentrifuge (Heraeus Fresco, Thermo Fisher Scientific Inc., Waltham) for 5 min at 17,000 g and 4 °C, and then the supernatant was transferred into a fresh reaction tube. To the resulting soil pellet 700 µL of buffer PBL (5 mM Tris-HCl (pH 5), 5 mM Na₂EDTA, and 0.1% [wt/vol] sodium dodecyl sulfate) were added, and the disruption process was performed again as described above. Both supernatants from the lysis processes were pooled in one reaction tube.

The pooled supernatant was immediately extracted, initially with the addition of 500 µl of phenol/chloroform/isoamyl alcohol (25:24:1) and subsequent with chloroform/isoamyl alcohol (24:1). Afterwards, each time the sample was centrifuged for 5 min at 17,000 g and 4 °C. The resulting upper aqueous phase was transferred to a new reaction tube, 800 µl of PEG solution was added (30% [wt/vol]

polyethylene glycol 6000 and 1.6 M NaCl), incubated in ice for 30 min and centrifuged for 30 min at 17,000 g and 4 °C. Subsequently, the DNA/RNA pellet was washed with 800 µl of ice-cold 75% ethanol, dried out and dissolved in 50 µl of nuclease free water.

After extraction, samples were treated for DNA digestion with RNase-Free DNase Set (QIAGEN GmbH — Germany) according to manufacturer instructions; DNase reaction was stopped with 10 µl of 50 mM EDTA. With the DNA-free RNA, a PCR was carried out, using the universal 16S rRNA gene primers 27F (5'-AGAGTTTGATCMTGGATCMTGGCTCAG-3') and 1492R (5'-GGTTACCTTGTTACGACTT-3') [48, 49] and checked on agarose gel electrophoresis to verify the absence of remaining DNA in the samples. Subsequently, reverse transcription was performed utilizing AccuScript High Fidelity 1st Strand cDNA Synthesis Kit (Agilent Technologies, Inc., Cedar Creek, TX, USA) following manufacturer instructions.

16S rRNA Ion Torren Sequencing and Metabarcoding Analysis

The 16S rRNA gene hypervariable regions (V4&V5) were PCR amplified using the set of primers 520F (5'-AYTGGGYDTAAAGNG-3') [50] and 907R (5'-CCGTCAATTCMTTTRAGTTT-3') [51] and sequenced by Ion Torrent technique following the protocol described by Kaplan et al. [52]. The obtained Ion Torrent sequencing output was analyzed using QIIME2 version 2020.6.0 [53], sequences were demultiplexed with the QIIME2 cutadapt command [54] using a barcode error rate of 0 and assigned to specific samples by corresponding barcodes. Later, quality control, denoising, sequences dereplication, and chimera filtering were performed using DADA2 software [55]; the first 15 nucleotides were trimmed, and sequences were truncated at a position of 320 nucleotides. Amplicon sequence variants (ASV) generated with DADA2 were taxonomically affiliated with a trained fitted classifier [56, 57] based on the SILVA 138 database [58, 59].

Alpha and beta diversity analyses were performed using R studio software 1.1.419, R packages Phyloseq 1.22.3 [60] and Vegan 2.4–6 [61]. Before diversity analyses, ASVs were collapsed by genera. For alpha diversity assessment, rarefaction was applied and diversity indices (Observed species, Simpson, Shannon, Fisher) were calculated and compared among CO₂ conditions and soil habitats using the Wilcoxon test [62] with the Bonferroni correction method through 999 permutations. For non-constrained beta diversity analyses, data were transformed using centered log ratio (clr) method [63, 64], using R package Aldex2 1.18.0 [65]. Later, community dissimilarity distance matrices were created using the Aitchison distance [63, 64] and visualized using principal component analysis (PCA) [66]. Statistical differences

among treatments, rings, and CO₂ conditions were assessed by a permutational multivariate analysis of variance using Adonis method and employing 999 permutations [67]. Additionally, the degree of dispersion of the bacterial community composition from the four soil cores taken in each ring was assessed as described above. Redundancy analysis (RDA) was used to explore associations between microbial community structures and environmental parameters, and a permutation test of redundancy analysis using 999 permutations was applied for evaluating their statistical significance [68].

For the analysis of correlation between bacterial genera and environmental parameters, the genera belonging to the core microbiome of each of the soil sample groups were calculated, and their counts were transformed to relative abundance with package Microbiome version 1.8.0 [69]. Later, core microbiomes were calculated including genera with a total relative abundance of $\geq 0.01\%$ and present in $\geq 85\%$ of the corresponding group's samples. A correlation test was performed using Aldex2 1.18.0 [65] and its "aldex.corr" function, utilizing Pearson's correlation coefficient, and p values were corrected using false discovery rate (FDR) method with an alpha of < 0.05 .

Differential abundance of genera from rhizosphere soils was assessed by comparing the core microbiomes of each CO₂ condition utilizing the R packages DESeq2 1.24.0 [70] and Aldex2 1.18.0 [65]. DESeq2 analysis was performed by estimating the size factor and the dispersion using the geometric mean of the core microbiome genera; later, values were fitted with a generalized linear model using negative binomial distribution and applying a Wald significance tests, the option "local" for fitting of dispersions to the mean intensity and an alpha threshold of < 0.05 . Aldex2 analysis was done by performing a centered log ratio (clr) transformation using as denominator the geometric mean abundance of all features and 128 Monte Carlo instances; later, a Welch's t-test with a Benjamini–Hochberg correction and threshold < 0.05 was performed.

Functional capabilities based on the obtained 16S rRNA data were predicted using PICRUSt2 version (v2.3.0 beta) [71]. PICRUSt2 analysis was carried out using the default pipeline option. Afterward, EC number, KO functions, and MetaCyc non-constrained beta diversity and differential abundance analyses were performed as described above.

Quantitative PCR

The quantification of 16S rRNA gene to estimate total bacterial abundance was performed following the protocol described by Kaplan et al. [52], but instead of DNA, cDNA products described above were used for the quantification. Quantitative PCR (qPCR) was conducted on a Rotor-Gene Q (Qiagen, Hilden, Germany) by using Absolute qPCR SYBR Green Mix (Thermo Fisher Scientific). Statistical

comparisons were done with Kruskal–Wallis and Wilcoxon tests with the Benjamini–Hochberg adjustment method using R Package stats version 3.6.3.

Results

Ion Torrent Sequencing

A total of 5,855,099 raw sequences were obtained. After demultiplexing, sequences were assigned to each sample, ranging sequence counts in each sample from 306,675 to 22,410. After quality control, denoising, sequence dereplication, and chimera filtering with DADA2 software, 2,674,159 sequences were removed, resulting in 3,180,940 non-chimeric sequences and 11,587 representative sequences which were grouped into ASVs (Amplicon sequence variations) at a 99% similarity. Later, sequences belonging to chloroplast and mitochondria were removed, resulting in 11,508 ASVs.

Soil Microbial Diversity

Diversity indexes were evaluated to assess differences in soil microbiome between eCO₂ and aCO₂ conditions. In the Gi-FACE, soil active bacterial diversity changed

due to the influence of increased concentrations of CO₂ (Fig. 1). These changes are better appreciated when comparing bulk and rhizosphere soil fractions from aCO₂ and eCO₂ rings separately. In regard to alpha diversity of rhizosphere and bulk soil fractions from aCO₂ rings, significantly higher diversity values were observed in bulk compared to rhizosphere soils with Observed species (p value 0.00036), Shannon (p value 0.0086), and Fisher (p value 0.00036) indexes (Fig. 1). Nevertheless, this difference was not detected between bulk and rhizosphere soil fractions from eCO₂ rings, indicating an evenness between the rhizosphere and bulk soils in eCO₂ rings (Fig. 1). Likewise, eCO₂ rhizosphere soil presented greater diversity values in comparison to its aCO₂ counterpart, according to Observed species (p value 0.0193) and Fisher (p value 0.0193) indexes.

A distance matrix was created using the Aitchison distance and later ordinated using the principal component analysis (PCA) to further analyze the microbiome composition. Initially, the dispersion of the four soil cores taken within each ring and their distance to the centroids was assessed. They indicated a considerably different soil microbiome composition in each soil core, even when soil cores of the same rings were compared (S1). On the other hand, the assessment of differences among the evaluated habitats showed that the strongest effect on the bacterial microbiome

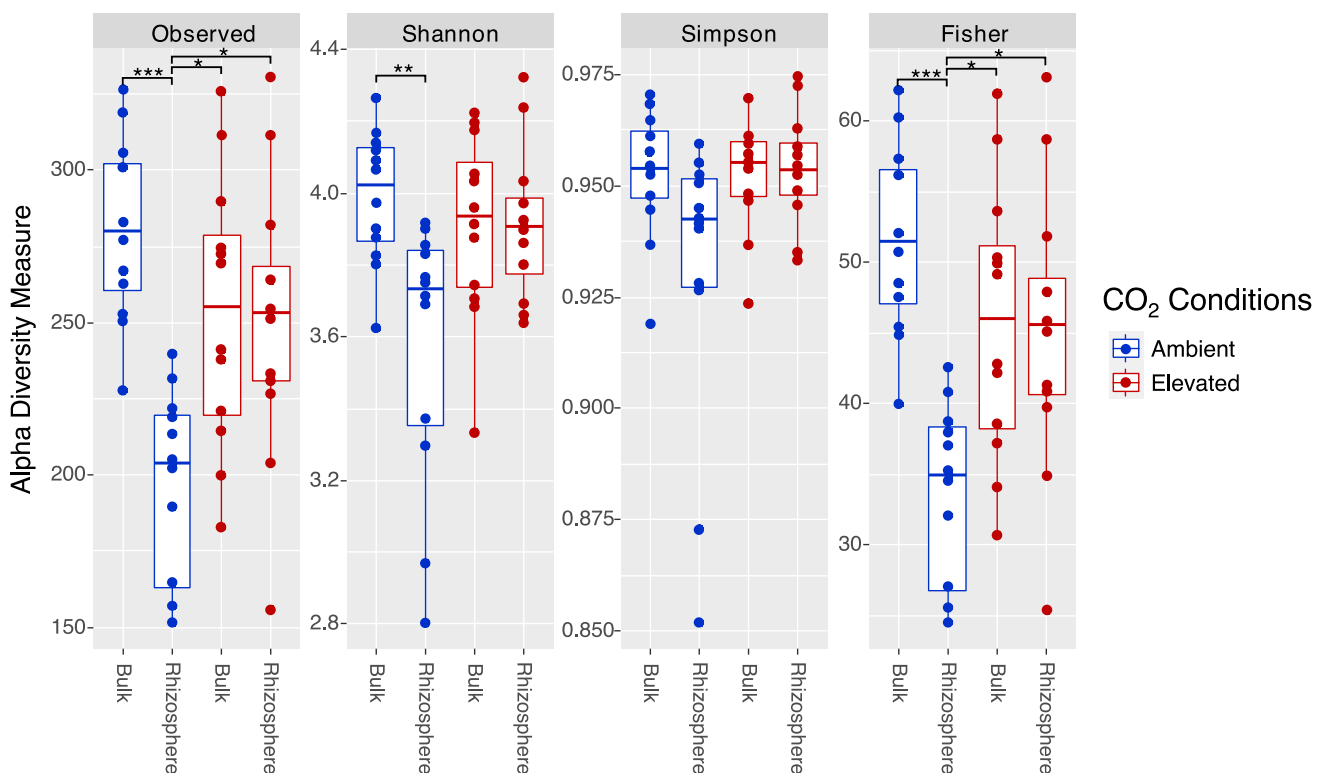


Fig. 1 Alpha diversity metrics. aCO₂, ambient CO₂ conditions; eCO₂, elevated CO₂ conditions. * p smaller 0.01, ** p smaller 0.001, *** p smaller 0.0001

differentiation in the soil was the ring factor, either for rhizosphere or bulk soils (p value 0.001).

Similarly, there were significant differences among the community composition of the four evaluated groups (aCO₂ bulk soil, aCO₂ rhizosphere soil, eCO₂ bulk soil, eCO₂ rhizosphere soil) (p value 0.001). In the same way, the PCA showed a clear differentiation between the microbiome composition of the rhizospheres from eCO₂ and aCO₂ rings (p value 0.002) (Fig. 2a). On the contrary, the separation of the microbial community composition between the bulk soils from aCO₂ and eCO₂ rings was not clear and statistically not significant (p value 0.327) (Fig. 2b).

Effect of Environmental Parameters on Microbial Community

A redundancy analysis (RDA) was carried out to assess the effect of environmental factors on the soil microbiome of the Gi-FACE. The results indicated that continuously higher

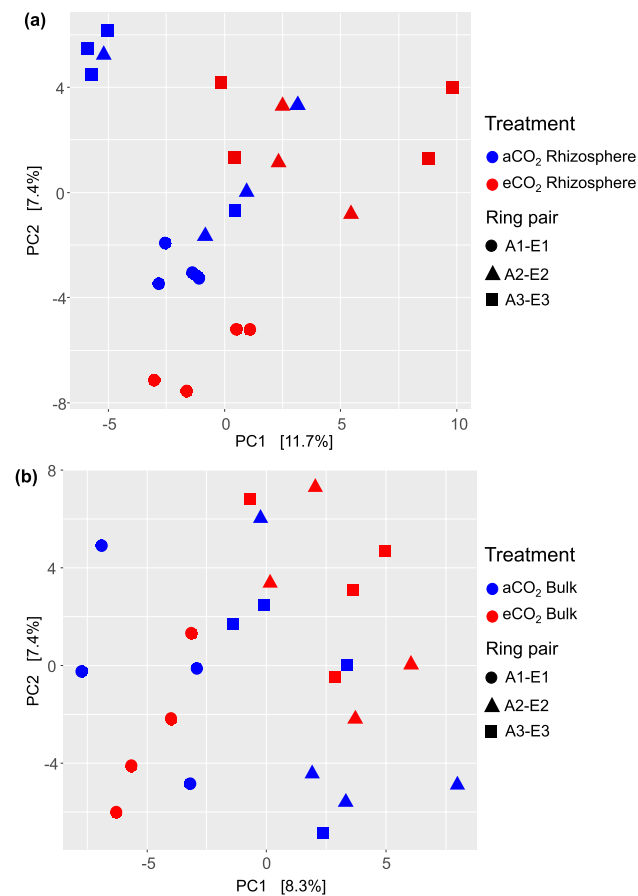


Fig. 2 Principal component analysis (PCA) calculated based on Aitchison community dissimilarity distance matrix of **a** rhizosphere soils from ambient and elevated CO₂ rings and **b** bulk soils from ambient and elevated CO₂ rings. A, ambient CO₂ rings; E, elevated CO₂ rings; aCO₂, ambient CO₂ conditions; eCO₂, elevated CO₂ conditions

environmental CO₂ concentration was a factor that exerted a significant effect on the differentiation of the microbial communities of eCO₂ rings (p value 0.021) (Table 1, Fig. 3a). Furthermore, CO₂ soil fluxes on average were 35% higher in eCO₂ rings in comparison to the aCO₂ ones, and this difference was statistically significant throughout the assessed period of time (p value 0.031) (Fig. 3b). Moreover, increased soil fluxes of CO₂ are associated with the differences that were observed in Gi-FACE soil microbiome (p value 0.001).

Likewise, the ammonium content in the whole soil, rhizosphere and bulk soil fractions had a significant influence on the community composition (Table 1), despite the fact that soil ammonium concentrations were not significantly different between eCO₂ and aCO₂ rings (p value 0.313) (S2). Similarly, the total carbon content had significant influence on the whole soil and bulk soil microbial community structure (Table 1), but likewise ammonium there were no significant differences in carbon content between aCO₂ and eCO₂ rings (p value 0.1304) (S2). On the contrary, the average carbon/nitrogen ratio in the whole soil of the eCO₂ rings (11.1:1) was significantly higher in comparison with aCO₂ rings (10.69:1) (p value 0.0069) and had a significant effect (p value 0.025) on the microbial community composition (Table 1).

Furthermore, when observing each habitat separately, the RDA indicated that in the rhizosphere soil, the CO₂ atmospheric concentration had a significant effect on the microbiome differentiation between the aCO₂ and eCO₂ rings (p value 0.010) (Table 1, Fig. 3c). In contrast, eCO₂ had no substantial influence on the composition of the microbial community's structure of the bulk soils (p value 0.097) (Table 1, Fig. 3d).

Correlation analysis between environmental variables and rhizosphere soil core microbiome demonstrated that the abundance of several bacterial genera was either positively or negatively correlated with environmental CO₂ concentrations and soil CO₂ fluxes. Among the main bacterial families that were significantly positively correlated

Table 1 p values of permutation test for redundancy analysis (RDA) under reduced model using an Aitchison community dissimilarity distance matrix

Environmental parameter	Whole soil	Rhizosphere soil	Bulk soil
C:N	0.025 *	—	0.127
CO ₂ injected concentration	0.021 *	0.010 **	0.097
CO ₂ flux concentration	0.001 ***	0.003 **	0.004 **
NH ₄ ⁺	0.001 ***	0.002 **	0.018 *
Total carbon	0.001 ***	0.007 **	0.001 ***
Water holding capacity	0.006 **	0.024 *	0.100
Total nitrogen	0.141	—	0.688

Significance codes: 0.0001 '***', 0.001 '**', 0.01 '*'

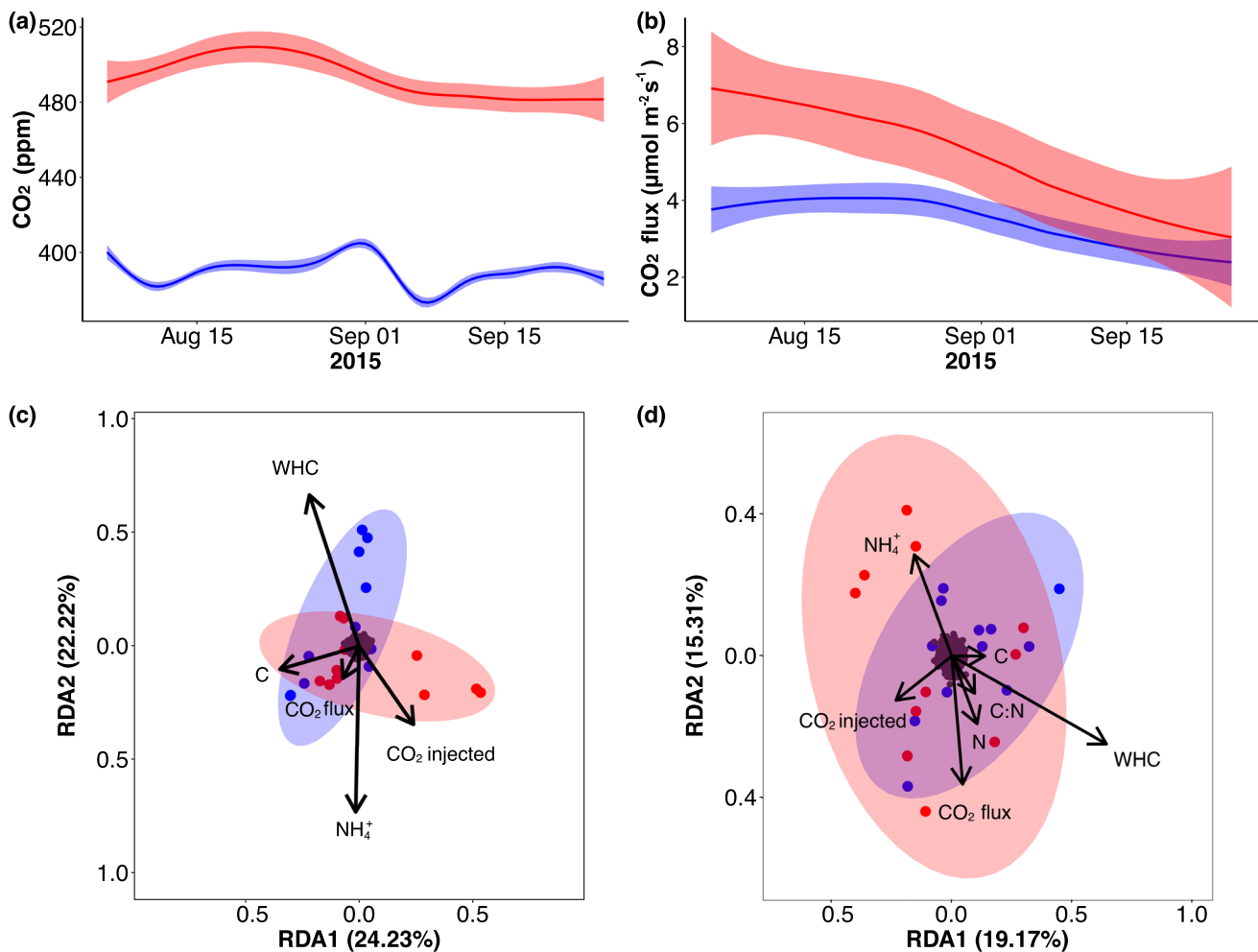


Fig. 3 Time series data from August to September 2015 of **a** average environmental CO₂ concentrations and **b** average soil CO₂ fluxes of ambient (blue) and elevated (red) CO₂ conditions; level of confidence interval of 0.95. Redundancy analysis (RDA) based on Aitchison

community dissimilarity distance matrix of **c** rhizosphere soils from ambient (blue) and elevated (red) CO₂ rings and **d** bulk soils from ambient (blue) and elevated (red) CO₂ rings; black dots indicate soil bacterial genera

with environmental eCO₂ and soil CO₂ fluxes concentrations are Rhodanobacteraceae, “Labraceae,” Xanthomonadaceae, Rhodobacteraceae, Rhizobiaceae, Pseudomonadaceae, Phaselicystidaceae, Haliangiaceae, Bacillaceae, Streptomycetaceae, Xanthobacteraceae, Burkholderiaceae, Devosiaceae, Haliangiaceae, Comamonadaceae and Polyangiaceae (Table S3.1). On the contrary, families “Solibacteraceae,” Caulobacteraceae, Acetobacteraceae, Thermoactinomycetaceae, Beijerinckiaceae, and Blastocatellaceae were negatively correlated with environmental eCO₂ and soil CO₂ fluxes (Table S3.1). Moreover, bacterial orders Nitrospirales, Caulobacterales, “Rokubacteriales,” Vicinamibacterales, “Tistrellales,” and “Rokubacteriales” were significantly correlated with NH₄⁺ content and soil water holding capacity in rhizosphere soils (Table S3.1).

Changes on the Rhizosphere Microbial Community Composition

Differential abundance analyses demonstrated that several rhizosphere soil genera were affected. Both Aldex2 and DESeq2 demonstrated that 42 bacterial genera were stimulated under eCO₂, among those are *Haliangium*, *Phaselicystis*, *Rhizobacter*, *Pseudomonas*, *Rhizobium*, *Phyllobacterium*, *Mesorhizobium*, *Rhodanobacter*, *Labrys*, unidentified genus of the class “Sericytochromatia,” *Dokdonella*, *Massilia*, *Burkholderia*, *Bacillus*, *Novosphingobium*, *Acidibacter*, and *Streptomyces* (Fig. 4a, Fig. 4b). These genera showed Log₂ Fold changes ranging from 0.910 to 9.67. Furthermore, Aldex2 test showed that other 56 genera were significantly stimulated in the rhizosphere soil of eCO₂ rings. These

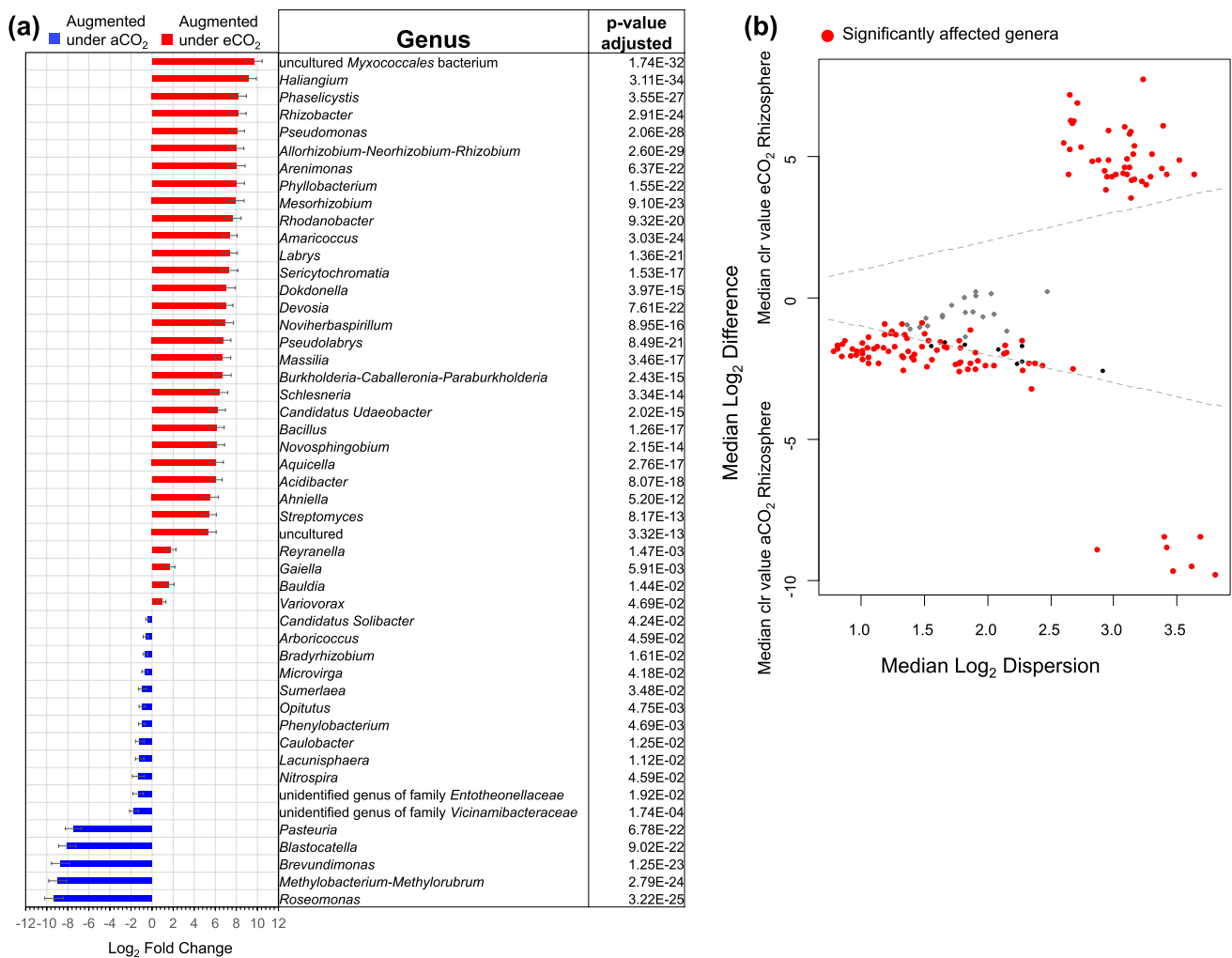


Fig. 4 Differential abundances of core microbiome bacterial genera of rhizosphere soil under elevated and ambient CO₂. **a** DESeq2 test results with an alpha threshold < 0.05 and error expressed as standard error of log fold change. **b** Aldex2 results using centered log ratio

genera belonged mainly to bacterial families Nocardioi-daceae, Beijerinckiaceae, Pyrinomonadaceae, “Koribacte-raceae”, “Xiphinematobacteraceae,” Propionibacteriaceae, Dongiaceae, Geminicoccaceae, Solirubrobacteraceae, Blastocatellaceae, Caulobacteraceae, Nitrosomonadaceae, Xanthobacteraceae, Caulobacteraceae, Fibrobacteraceae, Acetobacteraceae, unidentified family of the phylum “Latescibacterota,” Myxococcaceae, “Solibacteraceae”, Rhizobiaceae, and Gemmatimonadaceae (S3).

On the contrary, both differential abundance tests indicated that some genera presented a decreased of abundance under eCO₂ conditions. Among these are unidentified genus of the family Vicinamibacteraceae, *Pasteuria*, *Caulobacter*, unidentified genus of the family “Entotheonellaceae,” *Brevundimonas*, *Methylobacterium-Methylorubrum*, *Sumerlaea*, *Blastocatella*, *Phenylobacterium*, *Lacunisphaera*,

(clr) transformation and the geometric mean abundance of all features; red points indicate significantly different genera after Welch’s t-test and Benjamini–Hochberg correction with an alpha threshold < 0.1

Roseomonas, and *Opiritus*. These genera had Log₂ Fold changes from – 0.421 to – 9.31 in eCO₂ ring (Fig. 4a, Fig. 4b, S3).

Functional Metagenomics Prediction

Beta diversity results of functional capabilities based on 16S rRNA data showed significant differences on functional metagenome’s composition of rhizosphere soils from aCO₂ and eCO₂ conditions. PICRUSt2 predicted functional metagenome were different regarding Enzyme Commission number (EC number) (p value 0.005), KEGG Orthology (KO) for molecular functions (p value 0.019), and MetaCyc Metabolic Pathways (p value 0.022) (S4). Moreover, similar to taxonomical results, predicted bulk soil’s functional metagenomics from aCO₂ and eCO₂ conditions did not show

great differences regarding its beta diversity, neither on EC numbers (p value 0.197), KEGG Orthology (p value 0.179), or MetaCyc Metabolic Pathways (p value 0.317) (S4).

Besides, the analyses of significantly affected predicted enzymes indicated that several enzymes of degradation of carbon compounds were significantly stimulated in rhizospheric soils under eCO₂ conditions. Enzymes involved in carbohydrates, lipids, amino acids, and polycyclic aromatic hydrocarbon degradation were significantly stimulated. Additionally, numerous predicted enzymes and pathways of synthesis of cellular components, membrane transporters, and quorum sensing were significantly higher under eCO₂ conditions (S5). Also, according to KEGG Orthology for molecular functions, several enzymes involved in nitrogen fixation, nitric-oxide synthesis, and nitrite and nitrate reduction were predicted to be more abundant in eCO₂ rhizosphere soil (S5).

Quantitative PCR

Active biomass estimation by 16S rRNA quantification demonstrated changes due to eCO₂ concentrations. A 20% increase of 16S rRNA copy numbers per g dry weight soil in eCO₂ rhizosphere ($2.07 \pm 0.50 \cdot 10^8$) in comparison to aCO₂ rhizosphere ($1.66 \pm 0.44 \cdot 10^8$) was observed (p value 0.0001). Nevertheless, when comparing the 16S rRNA copy

numbers per gram dry weight soil of bulk soils from aCO₂ ($2.35 \pm 0.80 \cdot 10^8$) and eCO₂ ($2.35 \pm 0.79 \cdot 10^8$) conditions, no significant differences were found (p value 0.9588) (Fig. 5). Moreover, significant differences were found between bulk and rhizosphere soils from aCO₂ (p value $2.1 \cdot 10^{-5}$) with in average 29% more copies per dry weigh in bulk soil compared to rhizosphere soil. Nonetheless, when comparing rhizosphere and bulk soils from eCO₂ rings, this difference is lower and not significant (p value 0.1455), with the bulk soil having 12% more copies than the rhizosphere soil (Fig. 5).

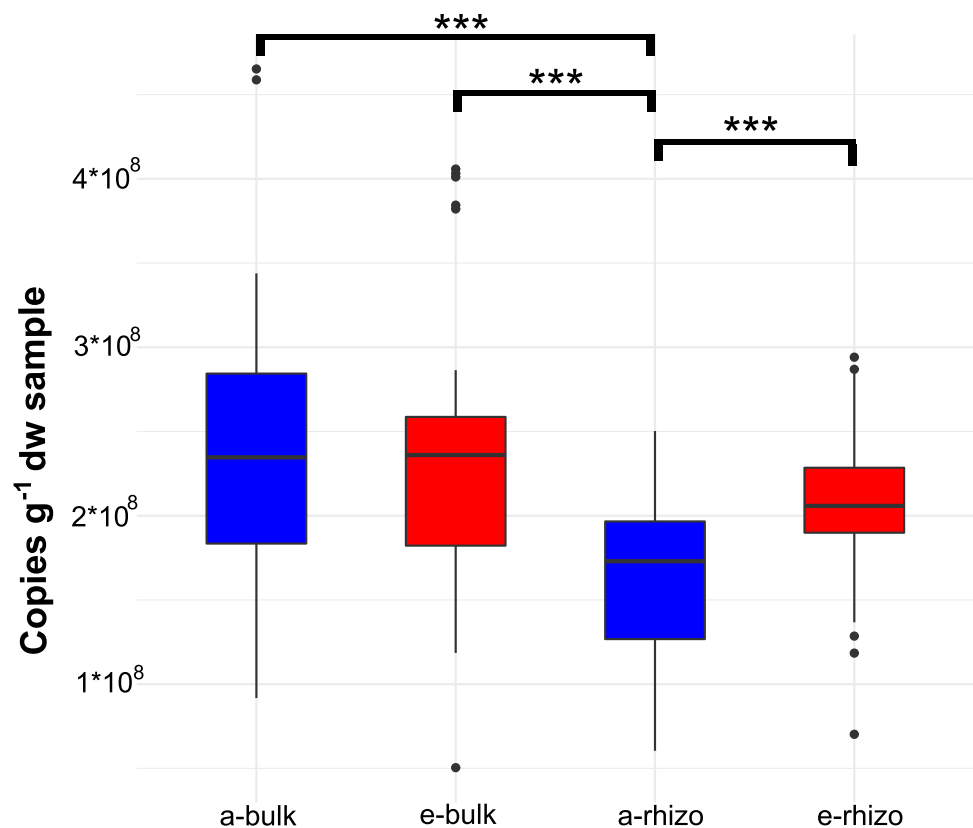
Discussion

Changes in Microbiome Structure and Composition

Elevated CO₂ concentrations affect the composition and biomass of soil microbial communities in the rhizosphere because of greater inputs of labile carbon (C) via root exudation may increase the microbial N demand. This causes an increased competition between plants and soil microorganisms for available N; therefore, N dynamics are likely to change under eCO₂ [10, 11, 14, 72].

Our results showed that eCO₂ had a strong effect in the Gi-FACE on the metabolic active microbiome of the rhizosphere soil, in contrast to the microbiome of the bulk soil

Fig. 5 Boxplot of 16S rRNA quantification of ambient CO₂ rings bulk soil (a-bulk), elevated CO₂ rings bulk soil (e-bulk), ambient CO₂ rings rhizosphere soil (a-rhizo) and elevated CO₂ rings rhizosphere soil (e-rhizo). Significance codes: 0.0001 '***'



which remained mostly unaffected. Alpha diversity indices indicate that a shift occurred under eCO₂ conditions, producing an evenness in terms of alpha diversity between rhizosphere and bulk soil. Since significant differences were found between bulk and rhizosphere soil of aCO₂ rings, this evenness represents an increase in alpha diversity of eCO₂ rhizosphere soil (Fig. 1). Furthermore, beta diversity results revealed a different abundance and microbial community composition in the rhizosphere of eCO₂ rings compared to aCO₂ rings (Fig. 2).

These results differ from previous reports of the eCO₂ effects on the Gi-FACE soil microbiome, which stated that only subtle or no effect occurred on microbial communities and that the differences were mostly due to soil conditions and the moisture gradient that occurs at this facility [25–27]. Similarly, to the aforementioned studies, our data confirmed that samples from ring-pair A1-E1 had lower water content in comparison to A2-E2 and A3-E3 samples (S2), and that water holding capacity (WHC) significantly influenced the soil microbiome (Table 1, Fig. 3). This was observable in the effect that the ring-pair factor had on the beta diversity of the Gi-FACE soil microbiome (p value 0.001) (Fig. 2).

Nonetheless, besides the moisture gradient, the observed differences caused by the eCO₂ were likely detected due to the RNA-based metabarcoding approach used in our work, which is able to differentiate the metabolic active microorganisms from the inactive ones, avoiding the biases caused by DNA of dead cell or extracellular DNA, which can comprise approximately 41% of the amplifiable prokaryotic 16S rRNA genes in soil [31]. However, RNA metabarcoding has its limitations as well, mainly due to the fact that RNA conversion to cDNA requires the use of a reverse transcriptase which lacks proofreading activity, creating point mutations in some of the cDNA sequences [73]. Reverse transcriptase also regularly performs template switching, which can lead to the production of chimeric cDNA sequences and the creation of shortened isoform sequences from intramolecular template switching [74, 75]. Nevertheless, in our study these limitations were minimized by using a Moloney murine leukemia virus reverse transcriptase (MMLV-RT) derivative combined with a *E. coli* DNA polymerase III ϵ subunit which lowers the reverse transcription error rate by threefold, and later the resulting cDNA was amplified with a proofreading DNA polymerase which produced up to eightfold fewer errors [76].

The study of Bei et al. [28], which also addressed the active microbial community by using a metatranscriptomic approach, supports our results. For the summer of 2015, the same year that we took the samples for this study, they reported significant effects of eCO₂ on the functional expression related to rhizosphere and plant roots associated microbiomes in the Gi-FACE. Also, similarly to our work, they described that the increase in bacterial abundance was

related to significant enrichment of different taxonomical groups, including Acidobacteria, Actinobacteria, and Proteobacteria, and changes related to a significant decrease in Fungi and increase in Actinobacteria.

However, Bei et al. [28] found no significant eCO₂ effect on the rhizosphere soil and root-associated microbiomes during the summer of 2017. These contrasting results for different years may result from climatic conditions in summer, since the summer 2015 was characterized by prolonged heat waves, while the mean temperature in summer 2017 was closer to the long-term average. The effect of eCO₂ on the soil rhizosphere microbiome we found in our study may be affected by the above average temperatures of this particular year. Additionally, the prediction that heat waves will occur more frequently in the future [77] emphasizes the importance of our findings.

The reason why only the rhizosphere microbiome, in contrast to the bulk soil microbiome, was affected by eCO₂ influx is most probably a consequence of the priming effect of the increased flux of roots exudates and consequently higher availability of carbon compounds. This increased supply of labile C causes an accelerated decomposition of soil organic C [15], which activates previously dormant microorganisms [15, 16].

Effect of eCO₂ Concentration on Microbial Community, C and N Cycles

Our results of the effect of environmental parameters on soil microbiome composition demonstrated that several rhizosphere bacterial families such as Rhodanobacteraceae, “Labraceae,” Xanthomonadaceae, Rhodobacteraceae, Rhizobiaceae, Pseudomonadaceae, Phaselicystidaceae, Haliangiaceae, Bacillaceae, Streptomycetaceae, Xanthobacteraceae, Burkholderiaceae, Devosiaceae, Haliangiaceae, Comamonadaceae, and Polyangiaceae were positively correlated with eCO₂ fumigation and soil CO₂ fluxes. Within these families are found bacterial genera as *Streptomyces*, *Burkholderia*, *Dokdonella*, *Bacillus*, *Pseudolabrys*, *Devosia*, *Mesorhizobium*, *Acidibacter*, *Rhizobacter*, *Rhodanobacter*, *Arenimonas*, *Amaricoccus*, *Phyllobacterium*, *Rhizobium*, *Pseudomonas*, *Phaselicystis*, and *Haliangium*. Furthermore, the aforementioned genera had significant higher counts under eCO₂ conditions according to DESeq2 and Aldex2 results. From other experiments, it was also reported that under eCO₂ conditions the rhizosphere soil microbial communities had changed [78]. Increased atmospheric CO₂ concentrations could also change the competitive ability of *Rhizobium leguminosarum* bv. *trifolii*, probably due to changes in root exudates [79]. In salt marsh systems containing the halophyte *Suaeda japonica*, it was reported that gene abundances and microbial community structures were both affected by eCO₂, and rhizospheric microorganisms

responded to eCO₂ more strongly than those inhabiting the bulk soil [80]. Song et al. [81] described that community composition of soil microbiota associated with *Phytolacca americana* and *Amaranthus cruentus* roots were significantly affected by eCO₂, and numbers of bacteria and fungi, as well as microbial C and N in the rhizosphere soils of both species, were higher at eCO₂.

Greater carbon input due to eCO₂ also explains the increase of 35% in soil CO₂ fluxes and the 20% augmentation in 16S rRNA copy numbers from active bacterial biomass observed in rhizosphere soil under eCO₂ in comparison to aCO₂, which corresponded to an increased soil biological activity in Gi-FACE. Cheng et al. [82] described that eCO₂ affected soil microbial respiration, producing an augmentation of microbial biomass and activities. Similarly, King et al. [83] showed that eCO₂ increased soil respiration at four forest FACE experiments. Blagodatskaya et al. [84] demonstrated that augmented available organic C released by roots at eCO₂ altered the ecological strategy of the soil microbial community, occurring a shift to a higher contribution of fast-growing species. The increased biological activity in eCO₂ rhizosphere soil is supported by the predicted functional metagenome obtained with PICRUSt2, which shows significant increases in several enzymes involved in cellular components biosynthesis such as peptidoglycan, lipopolysaccharide, amino acids, bacterial motility proteins, and lipids synthesis (S5). These results differ from those obtained by Pujol Pereira et al. [23], who reported that on soybean [*Glycine max* (L.) Merr.], eCO₂ decreased 16S rRNA gene abundance in rhizosphere soil by 31%. Also, Marhan et al. [21] described that abundances of total 16S rRNA were not influenced by CO₂ but by sampling date and depth. Likewise, Brenzinger et al. [27] and Bei et al. [28] reported that at the Gi-FACE no differences between aCO₂ and eCO₂ rings were found regarding the 16S rRNA gene. However, Bei et al. [28] described that in summer of 2015 under eCO₂ conditions the functional metagenome of rhizosphere soil presented an increase on amino acids and carbohydrates metabolisms, membrane transporters, and quorum sensing proteins: similar to our study's PICRUSt2 results (S5).

In addition, several genera involved in the degradation of carbon (C) compounds were stimulated under eCO₂ conditions; among these are *Pseudomonas* and *Bacillus* (Fig. 4, S2) that have been previously reported to degrade lignocellulose materials. *Pseudomonas boreopolis* produces a cellulase-free xylanase with a high activity of hemicellulose degradation [85]. Maki et al. [86] reported that *Bacillus* strain (55S5) and a *Pseudomonas* strain (AS1) displayed high potential for lignocellulose decomposition due to a variety of cellulase and xylanase activities. Trujillo-Cabrera et al. [87] described the isolation of cellulolytic bacteria from high humus content soils, as

Bacillus thuringiensis and *Pseudomonas gessardii*. The augmentation of these taxa would agree with the predicted functional metagenome, which indicated an increment of several enzymes involved in lignocellulose materials degradation, as Chitinase (EC:3.2.1.14), Endo-1,3(4)-beta-glucanase (EC:3.2.1.6), Endo-1,4-beta-xylanase (EC:3.2.1.8), and Cellulase (EC:3.2.1.4) (S5). Similar results have been described by He et al. [17, 19], who reported that soils of a soybean agro-ecosystem and a glacial outwash sandplain showed increased abundance of encoding genes for enzymes involved in labile C degradation such as amylase, glucoamylase, pullulanase, fungal arabinofuranosidase, xylanase, endoglucanase, acetylglucosaminidase, and exochitinase. Likewise, Xiong et al. [20] described that alpha-amylase, cellobiase, endoglucanase, vanillin dehydrogenase, endochitinase, and phenoloxidase encoding genes were stimulated under eCO₂ in soybean and maize fields. The above-mentioned increase of C compounds degradation could occur as a response of greater C availability due to an increase of root exudates under eCO₂ conditions.

Moreover, these changes in the C influx could induce a reduction of available N in the soil ecosystem [24], which alters the N cycle and induces significant changes in soil biogeochemical characteristics in the rhizosphere, such as NO₃⁻, available K⁺, soil microbial biomass carbon (SMBC), and available PO₄²⁻ [78]. The aforementioned process could explain the higher carbon/nitrogen ratio found in our study in eCO₂ rings in comparison with ambient ones and might also explain why some genera involved in different processes of the nitrogen cycle were stimulated under eCO₂ conditions. Genera belonging to families Rhizobiaceae and Xanthobacteraceae as *Rhizobium*, *Mesorhizobium*, and *Phyllobacterium* have been extensively reported as nitrogen-fixing bacteria [88–90], and in our study presented Log₂ fold increases ranging from 6.78 to 8.04. Also, PICRUSt2 results indicate that functional orthologs of the enzyme nitrogenase (EC:1.18.6.1) were significantly augmented in eCO₂ rhizosphere soil (S5). This increase in the abundance of nitrogen-fixing bacteria could have occurred as response to N deficiency, which eventually became a limiting factor for biomass production under eCO₂. Similar results were reported by Li et al. [91], who described a 24% increment of ¹⁵N in mine tailing soils under eCO₂ and a dominance of uncultured nitrogen-fixing bacteria.

Aldex2 correlation results demonstrated a significant negative correlation between NH₄⁺ content and *Nitrospira* genus under eCO₂ conditions. Although NH₄⁺ values were not significantly different between aCO₂ and eCO₂, NH₄⁺ content was on average 10% higher in aCO₂ soils, which suggest that nitrification processes could have been affected due to elevated environmental CO₂. Alterations in nitrification process in the Gi-FACE have been already described by Müller et al. [72], who reported that eCO₂ reduced NH₄⁺ oxidation to NO₃⁻ by 25%.

Furthermore, several denitrifying genera as *Streptomyces*, *Rhodanobacter*, *Pseudomonas*, *Burkholderia*, and *Bacillus* were significantly stimulated in eCO₂ rhizospheric soil with Log₂ fold changes between 5.37 and 8.065 [92–96]. Additionally, predicted functional metagenome indicate that several orthologs involved in the denitrification process, as nitric-oxide synthase (NAD(P)H) (EC:1.14.13.165), nitrate reductase (EC:1.7.99.4), nitrite reductase (NO-forming) (EC:1.7.2.1), nitrite reductase (cytochrome; ammonia-forming) (EC:1.7.2.2), periplasmic nitrate reductase NapA (EC:1.7.99.-), and nitric oxide reductase NorD protein, have significantly greater abundance under eCO₂ conditions (S5).

In summary, our results demonstrate that in the Gi-FACE, the rhizosphere soil microbiome was significantly affected due to the influence of increased CO₂ concentrations alongside other environmental factors. The increment of carbon input due to eCO₂ possibly augmented labile carbon degradation in rhizosphere soil reflected by the increment of bacteria biomass and CO₂ soil emissions. The aforementioned processes could cause a nitrogen constraint, observed in the increment of the C:N ratio, and decreased of NH₄⁺, which likely triggered a shift in the rhizosphere soil microbiome with an increment of nitrogen fixing and denitrifying taxa. The observed increase of denitrifier genera might explain the increased N₂O fluxes under eCO₂ conditions, previously described in the Giessen FACE [27, 97, 98]. Similarly, our data support the results described by Moser et al. [98], who reported that under eCO₂ conditions, N₂O emissions were 1.79-fold higher and that the linear interpolations showed a 2.09-fold increase in N₂O emissions mostly because of the oxidation of organic N and incomplete reduction of NO₂⁻, emitting N₂O instead of N₂ (Fig. 6).

Our findings suggest that alterations in carbon cycle affects nitrogen cycle dynamics in grassland soils, due to changes on the microorganisms involved on the different processes of these cycles. Nonetheless, further analyses would be necessary to assess the Gi-FACE microbiome metatranscriptome of carbon and nitrogen cycles, how they are affected by eCO₂, and how this effect depends on ambient temperature regimes like summer heat waves.

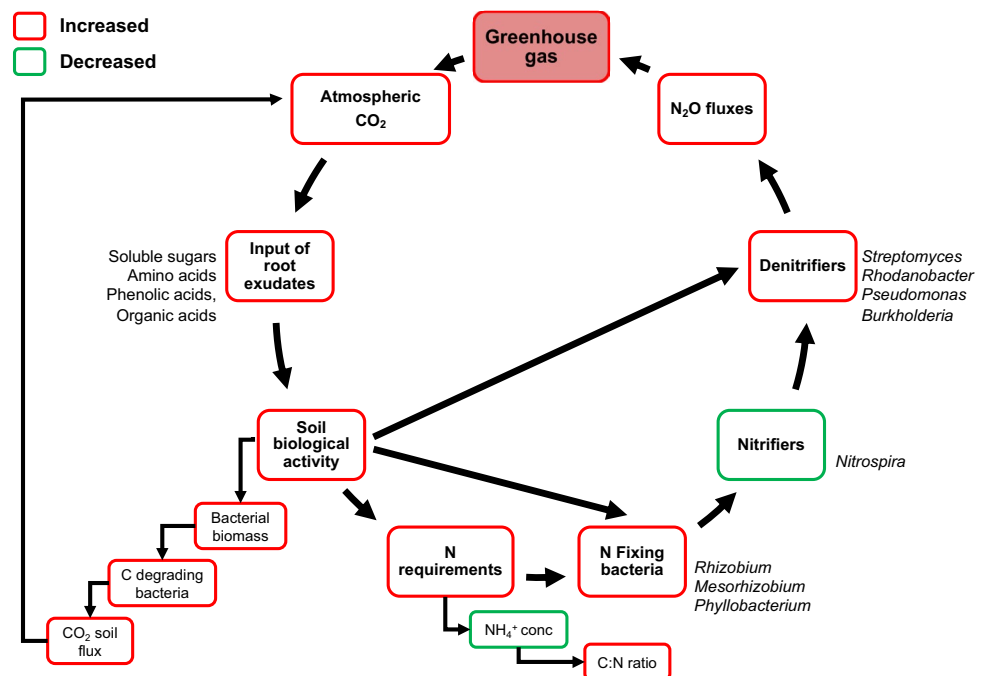
Supplementary Information The online version contains supplementary material available at <https://doi.org/10.1007/s00248-021-01791-y>.

Acknowledgements We thank Professor Bernd Honermeier group for their support to perform soil carbon and nitrogen analyses, and we are grateful to our colleagues Rita Geissler-Plaum and Bellinda Schneider for their excellent technical support. For the long-term funding of the Environmental Monitoring and Climate Impact Research Station Linden that enabled the long-term Gi-FACE experiment, we acknowledge the Hessian Agency for Nature Conservation, Environment and Geology (HLNUG).

Author Contribution DR conducted experiments, data curation, data analysis, and writing of the manuscript. SR contributed with methodology, review and editing. MC contributed with methodology, review and editing. CM conducted experiments and data curation. GM contributed with data curation, review and editing. MD conducted experiments, data curation, review and editing. Ch M contributed with methodology, review and editing. SS contributed with methodology, review and editing.

Funding Open Access funding enabled and organized by Projekt DEAL. This study was partially funded by the Environmental Monitoring and Climate Impact Research Station Linden that enabled the long-term Gi-FACE experiment and the Hessian Agency for Nature Conservation, Environment and Geology (HLNUG).

Fig. 6 Model diagram of the effect of elevated CO₂ on the rhizosphere microbiome of C and N cycles bacterial taxa of the Giessen FACE experiment



Data Availability The authors declare that the data supporting the findings of this study are available within the article and its Supplementary Information. cDNA sequence data are available in the GenBank database under the accession number PRJNA656997.

Code Availability Not applicable.

Declarations

Conflict of Interest The authors declare no competing interests.

Open Access This article is licensed under a Creative Commons Attribution 4.0 International License, which permits use, sharing, adaptation, distribution and reproduction in any medium or format, as long as you give appropriate credit to the original author(s) and the source, provide a link to the Creative Commons licence, and indicate if changes were made. The images or other third party material in this article are included in the article's Creative Commons licence, unless indicated otherwise in a credit line to the material. If material is not included in the article's Creative Commons licence and your intended use is not permitted by statutory regulation or exceeds the permitted use, you will need to obtain permission directly from the copyright holder. To view a copy of this licence, visit <http://creativecommons.org/licenses/by/4.0/>.

References

- IPCC (2014) Climate change 2014: Synthesis report. Contribution of working groups I, II and III to the fifth assessment report of the intergovernmental panel on climate change. IPCC, Geneva, Switzerland
- Idso K (1994) Plant responses to atmospheric CO₂ enrichment in the face of environmental constraints: a review of the past 10 years' research. *Agric For Meteorol* 69:153–203. [https://doi.org/10.1016/0168-1923\(94\)90025-6](https://doi.org/10.1016/0168-1923(94)90025-6)
- He P, Bader KP, Radunz A, Schmid GH (1995) Consequences of high CO₂ concentrations in air on growth and gas-exchange rates in Tobacco mutants. *Z Naturforsch* 50c:781–788
- Kimball BA (1983) Carbon dioxide and agricultural yield: An assemblage and analysis of 430 prior observations. *Agron J* 75:779. <https://doi.org/10.2134/agronj1983.00021962007500050014x>
- Owensby CE, Ham JM, Knapp AK et al (1997) Water vapour fluxes and their impact under elevated CO₂ in a C4-tallgrass prairie. *Glob Chang Biol* 3:189–195. <https://doi.org/10.1046/j.1365-2486.1997.00084.x>
- Kimball BA (2016) Crop responses to elevated CO₂ and interactions with H₂O, N, and temperature. *Curr Opin Plant Biol* 31:36–43. <https://doi.org/10.1016/j.pbi.2016.03.006>
- Habash DZ, Paul MJ, Parry MAJ et al (1995) Increased capacity for photosynthesis in wheat grown at elevated CO₂ - the relationship between electron transport and carbon metabolism. *Planta* 197:482–489. <https://doi.org/10.1007/BF00196670>
- Johnson RM, Pregitzer KS (2007) Concentration of sugars, phenolic acids, and amino acids in forest soils exposed to elevated atmospheric CO₂ and O₃. *Soil Biol Biochem* 39:3159–3166. <https://doi.org/10.1016/j.soilbio.2007.07.010>
- Jongen M, Jones MB, Hebeisen T et al (1995) The effects of elevated CO₂ concentrations on the root growth of *Lolium perenne* and *Trifolium repens* grown in a FACE* system. *Glob Chang Biol* 1:361–371
- Walker TS, Bais HP, Grotewold E, Vivanco JM (2003) Root exudation and rhizosphere Biology root exudation and rhizosphere biology. *Plant Physiol* 132:44–51. <https://doi.org/10.1104/pp.102.019661>. Although
- Li K, Guo XW, Xie HG et al (2013) Influence of root exudates and residues on soil microecological environment. *Pakistan J Bot* 45:1773–1779
- Phillips RP, Meier IC, Bernhardt ES et al (2012) Roots and fungi accelerate carbon and nitrogen cycling in forests exposed to elevated CO₂. *Ecol Lett* 15:1042–1049. <https://doi.org/10.1111/j.1461-0248.2012.01827.x>
- Jia X, Wang W, Chen Z et al (2014) Concentrations of secondary metabolites in tissues and root exudates of wheat seedlings changed under elevated atmospheric CO₂ and cadmium-contaminated soils. *Environ Exp Bot* 107:134–143. <https://doi.org/10.1016/j.envexpbot.2014.06.005>
- Dong J, Hunt J, Delhaize E et al (2021) Impacts of elevated CO₂ on plant resistance to nutrient deficiency and toxic ions via root exudates: a review. *Sci Total Environ* 754:142434. <https://doi.org/10.1016/j.scitotenv.2020.142434>
- Blagodatskaya E, Kuzyakov Y (2008) Mechanisms of real and apparent priming effects and their dependence on soil microbial biomass and community structure: critical review. *Biol Fertil Soils* 45:115–131. <https://doi.org/10.1007/s00374-008-0334-y>
- Di Lonardo DP, De Boer W, Klein Gunnewiek PJA et al (2017) Priming of soil organic matter: chemical structure of added compounds is more important than the energy content. *Soil Biol Biochem* 108:41–54. <https://doi.org/10.1016/j.soilbio.2017.01.017>
- He Z, Xu M, Deng Y et al (2010) Metagenomic analysis reveals a marked divergence in the structure of belowground microbial communities at elevated CO₂. *Ecol Lett* 13:564–575. <https://doi.org/10.1111/j.1461-0248.2010.01453.x>
- Xu M, He Z, Deng Y et al (2013) Elevated CO₂ influences microbial carbon and nitrogen cycling. *BMC Microbiol* 13:124. <https://doi.org/10.1186/1471-2180-13-124>
- He Z, Xiong J, Kent AD et al (2014) Distinct responses of soil microbial communities to elevated CO₂ and O₃ in a soybean agro-ecosystem. *ISME J* 8:714–726. <https://doi.org/10.1038/ismej.2013.177>
- Xiong J, He Z, Shi S et al (2015) Elevated CO₂ shifts the functional structure and metabolic potentials of soil microbial communities in a C4 agroecosystem. *Sci Rep* 5:1–9. <https://doi.org/10.1038/srep09316>
- Marhan S, Philippot L, Bru D et al (2011) Abundance and activity of nitrate reducers in an arable soil are more affected by temporal variation and soil depth than by elevated atmospheric [CO₂]. *FEMS Microbiol Ecol* 76:209–219. <https://doi.org/10.1111/j.1574-6941.2011.01048.x>
- Dunbar J, Gallegos-Graves LV, Steven B et al (2014) Surface soil fungal and bacterial communities in aspen stands are resilient to eleven years of elevated CO₂ and O₃. *Soil Biol Biochem* 76:227–234. <https://doi.org/10.1016/j.soilbio.2014.05.027>
- Pujol Pereira EI, Chung H, Scow K, Six J (2013) Microbial communities and soil structure are affected by reduced precipitation, but not by elevated carbon dioxide. *Soil Sci Soc Am J* 77:482. <https://doi.org/10.2136/sssaj2012.0218>
- Butterly CR, Phillips LA, Wiltshire JL et al (2016) Long-term effects of elevated CO₂ on carbon and nitrogen functional capacity of microbial communities in three contrasting soils. *Soil Biol Biochem* 97:157–167. <https://doi.org/10.1016/j.soilbio.2016.03.010>
- Regan K, Kammann C, Hartung K et al (2011) Can differences in microbial abundances help explain enhanced N₂O emissions in a permanent grassland under elevated atmospheric CO₂? *Glob Chang Biol* 17:3176–3186. <https://doi.org/10.1111/j.1365-2486.2011.02470.x>
- de Menezes AB, Müller C, Clipson N, Doyle E (2016) The soil microbiome at the Gi-FACE experiment responds to a moisture

- gradient but not to CO₂ enrichment. *Microbiology* 162:1572–1582. <https://doi.org/10.1099/mic.0.000341>
27. Brenzinger K, Kujala K, Horn MA et al (2017) Soil conditions rather than long-term exposure to elevated CO₂ affect soil microbial communities associated with N-cycling. *Front Microbiol* 8:1–14. <https://doi.org/10.3389/fmicb.2017.01976>
 28. Bei Q, Moser G, Wu X et al (2019) Metatranscriptomics reveals climate change effects on the rhizosphere microbiomes in European grassland. *Soil Biol Biochem* 138:1–10. <https://doi.org/10.1016/j.soilbio.2019.107604>
 29. Morrissey EM, McHugh TA, Preteska L et al (2015) Dynamics of extracellular DNA decomposition and bacterial community composition in soil. *Soil Biol Biochem* 86:42–49. <https://doi.org/10.1016/j.soilbio.2015.03.020>
 30. Dlott G, Maul JE, Buyer J, Yarwood S (2015) Microbial rRNA: RDNA gene ratios may be unexpectedly low due to extracellular DNA preservation in soils. *J Microbiol Methods* 115:112–120. <https://doi.org/10.1016/j.mimet.2015.05.027>
 31. Carini P, Marsden PJ, Leff JW et al (2016) Relic DNA is abundant in soil and obscures estimates of soil microbial diversity. *Nat Microbiol* 2:1–6. <https://doi.org/10.1038/nmicrobiol.2016.242>
 32. Felske A, Engelen B, Nübel U, Backhaus H (1996) Direct ribosome isolation from soil to extract bacterial rRNA for community analysis. *Appl Environ Microbiol* 62:4162–4167
 33. Duineveld BM, Kowalchuk GA, Keijzer A et al (2001) Analysis of bacterial communities in the rhizosphere of chrysanthemum via denaturing gradient gel electrophoresis of PCR-amplified 16S rRNA as well as DNA fragments coding for 16S rRNA. *Appl Environ Microbiol* 67:172–178. <https://doi.org/10.1128/AEM.67.1.172-178.2001>
 34. Hoshino YT, Matsumoto N (2007) DNA- versus RNA-based denaturing gradient gel electrophoresis profiles of a bacterial community during replenishment after soil fumigation. *Soil Biol Biochem* 39:434–444. <https://doi.org/10.1016/j.soilbio.2006.08.013>
 35. Hunt DE, Lin Y, Church MJ et al (2013) Relationship between abundance and specific activity of bacterioplankton in open ocean surface waters. *Appl Environ Microbiol* 79:177–184. <https://doi.org/10.1128/AEM.02155-12>
 36. Jäger HJ, Schmidt SW, Kammann C et al (2003) The University of Giessen free-air carbon dioxide enrichment study: description of the experimental site and of a new enrichment system. *J Appl Bot* 77:117–127
 37. Andresen LC, Yuan N, Seibert R et al (2018) Biomass responses in a temperate European grassland through 17 years of elevated CO₂. *Glob Chang Biol* 24:3875–3885. <https://doi.org/10.1111/gcb.13705>
 38. Kandeler E, Gerber H (1988) Short-term assay of soil urease activity using colorimetric determination of ammonium. *Biol Fertil Soils* 6:68–72. <https://doi.org/10.1007/BF00257924>
 39. Bak F, Scheff G, Jansen KH (1991) A rapid and sensitive ion chromatographic technique for the determination of sulfate and sulfate reduction rates in freshwater lake sediments. *FEMS Microbiol Lett* 85:23–30. <https://doi.org/10.1111/j.1574-6968.1991.tb04694.x>
 40. Forster JC (1995) Methods in Applied Soil Microbiology and Biochemistry. In: Alef K, Nannipieri P (eds) *Methods in applied soil microbiology and biochemistry*. Academic Press, San Diego, pp 105–106
 41. HBU (1996) *Handbuch der Bodenuntersuchung (HBU), Bodenbeschaffenheit - Bestimmung von organischem Kohlenstoff und Gesamtkohlenstoff nach trockener Verbrennung (Elementaranalyse)*. In: DIN ISO 10. GmbH, Berlin, p 3.4.1.31.1a
 42. VDLUFA (2012) *Methodenbuch- Band I, Die Untersuchung von Böden*, 6. VDLUFA - Verlag, Darmstadt
 43. Keidel L, Kammann C, Grünhage L et al (2015) Positive feedback of elevated CO₂ on soil respiration in late autumn and winter. *Biogeosciences* 12:1257–1269. <https://doi.org/10.5194/bg-12-1257-2015>
 44. Mirman D (2014) Growth curve analysis and visualization using R, 1st ed. Chapman and Hall/CRC in R series, Boca Raton
 45. Geller J, Winn MB, Mahr T, Mirman D (2020) GazeR: a package for processing gaze position and pupil size data. *Behav Res Methods* 52:2232–2255. <https://doi.org/10.3758/s13428-020-01374-8>
 46. Bates D, Mächler M, Bolker BM, Walker SC (2015) Fitting linear mixed-effects models using lme4. *J Stat Softw* 67:1–41. <https://doi.org/10.18637/jss.v067.i01>
 47. Mettel C, Kim Y, Shrestha PM, Liesack W (2010) Extraction of mRNA from soil. *Appl Environ Microbiol* 76:5995–6000. <https://doi.org/10.1128/AEM.03047-09>
 48. Lane DJ (1991) 16S/23S rRNA sequencing. In Stackebrandt E, Goodfellow M (eds) *Nucleic acid techniques in bacterial systematics*. John Wiley and Sons, New York, pp 115–175
 49. Weisburg WG, Barns SM, Pelletier DA, Lane DJ (1991) 16S Ribosomal DNA amplification for phylogenetic study. *J Bacteriol* 173:697–703
 50. Claesson MJ, O'Sullivan O, Wang Q et al (2009) Comparative analysis of pyrosequencing and a phylogenetic microarray for exploring microbial community structures in the human distal intestine. *PLoS ONE* 4:e6669. <https://doi.org/10.1371/journal.pone.0006669>
 51. Engelbrektson A, Kunin V, Wrighton KC et al (2010) Experimental factors affecting PCR-based estimates of microbial species richness and evenness. *ISME J* 4:642–647. <https://doi.org/10.1038/ismej.2009.153>
 52. Kaplan H, Ratering S, Felix-Henningsen P, Schnell S (2019) Stability of in situ immobilization of trace metals with different amendments revealed by microbial ¹³C-labelled wheat root decomposition and efflux-mediated metal resistance of soil bacteria. *Sci Total Environ* 659:1082–1089. <https://doi.org/10.1016/j.scitotenv.2018.12.441>
 53. Bolyen E, Rideout JR, Dillon MR et al (2019) Reproducible, interactive, scalable and extensible microbiome data science using QIIME 2. *Nat Biotechnol* 37:852–857. <https://doi.org/10.1038/s41587-019-0209-9>
 54. Martin M (2011) Cutadapt removes adapter sequences from high-throughput sequencing reads. *EMBnet J* 17:10
 55. Callahan BJ, McMurdie PJ, Rosen MJ et al (2016) DADA2: High-resolution sample inference from Illumina amplicon data. *Nat Methods* 13:581–583. <https://doi.org/10.1038/nmeth.3869>
 56. Pedregosa F, Varoquaux G, Gramfort A et al (2011) Scikit-learn: machine learning in python. *J Mach Learn Res* 12:2825–2830. <https://doi.org/10.1145/2786984.2786995>
 57. Bokulich NA, Kaehler BD, Rideout JR et al (2018) Optimizing taxonomic classification of marker-gene amplicon sequences with QIIME 2's q2-feature-classifier plugin. *Microbiome* 6:1–17. <https://doi.org/10.1186/s40168-018-0470-z>
 58. Quast C, Pruesse E, Yilmaz P et al (2013) The SILVA ribosomal RNA gene database project: Improved data processing and web-based tools. *Nucleic Acids Res* 41:590–596. <https://doi.org/10.1093/nar/gks1219>
 59. Glöckner FO, Yilmaz P, Quast C et al (2017) 25 years of serving the community with ribosomal RNA gene reference databases and tools. *J Biotechnol* 261:169–176. <https://doi.org/10.1016/j.jbiotec.2017.06.1198>
 60. McMurdie PJ, Holmes S (2013) Phyloseq: an R package for reproducible interactive analysis and graphics of microbiome census data. *PLoS ONE* 8:e61217. <https://doi.org/10.1371/journal.pone.0061217>

61. Oksanen J, Blanchet FG, Friendly M et al (2018) vegan: Community ecology package. R package version 2.5-7. <https://CRAN.R-project.org/package=vegan>
62. Wilcoxon F (1945) Individual comparisons of grouped data by ranking methods. *Biometrics Bull* 1:80–83. <https://doi.org/10.1093/jee/39.2.269>
63. Aitchison J (1982) The statistical analysis of compositional data. *J of the R Stat Soc Ser B* 44:139–177. <https://doi.org/10.1007/978-94-009-4109-0>
64. Aitchison J (1986) Book review, XII. Chapman and Hall, London
65. Fernandes AD, Macklaim JM, Linn TG et al (2013) ANOVA-like differential expression (ALDEx) analysis for mixed population RNA-Seq. *PLoS ONE* 8:e67019. <https://doi.org/10.1371/journal.pone.0067019>
66. Jolliffe IT, Cadima J (2016) Principal component analysis: a review and recent developments subject areas. *PhilTransRSocA* 374:1–16
67. Anderson MJ (2001) A new method for non parametric multivariate analysis of variance. *Austral Ecol* 26:32–46. <https://doi.org/10.1111/j.1442-9993.2001.01070.pp.x>
68. Legendre P, Oksanen J, ter Braak CJF (2011) Testing the significance of canonical axes in redundancy analysis. *Methods Ecol Evol* 2:269–277. <https://doi.org/10.1111/j.2041-210X.2010.00078.x>
69. Lahti L, Shetty S (2019) microbiome R package. <http://microbiome.github.io>
70. Love MI, Huber W, Anders S (2014) Moderated estimation of fold change and dispersion for RNA-seq data with DESeq2. *Genome Biol* 15:550. <https://doi.org/10.1186/s13059-014-0550-8>
71. Douglas GM, Maffei VJ, Zaneveld J et al (2019) PICRUSt2 for prediction of metagenome functions. *Nat Biotechnol* 38:669–673. <https://doi.org/10.1038/s41587-020-0550-z>
72. Müller C, Rütting T, Abbasi MK et al (2009) Effect of elevated CO₂ on soil N dynamics in a temperate grassland soil. *Soil Biol Biochem* 41:1996–2001. <https://doi.org/10.1016/j.soilbio.2009.07.003>
73. Houseley J, Tollervey D (2010) Apparent non-canonical trans-splicing is generated by reverse transcriptase in vitro. *PLoS ONE* 5:e12271. <https://doi.org/10.1371/journal.pone.0012271>
74. Cocquet J, Chong A, Zhang G, Veitia RA (2006) Reverse transcriptase template switching and false alternative transcripts. *Genomics* 88:127–131. <https://doi.org/10.1016/j.ygeno.2005.12.013>
75. Larocche O, Wood SA, Tremblay LA et al (2017) Metabarcoding monitoring analysis: the pros and cons of using co-extracted environmental DNA and RNA data to assess offshore oil production impacts on benthic communities. *PeerJ* 5:e3347. <https://doi.org/10.7717/peerj.3347>
76. Arezi B, Hogrefe HH (2007) *Escherichia coli* DNA polymerase III ϵ subunit increases Moloney murine leukemia virus reverse transcriptase fidelity and accuracy of RT-PCR procedures. *Anal Biochem* 360:84–91. <https://doi.org/10.1016/j.ab.2006.10.009>
77. Russo S, Sillmann J, Fischer EM (2015) Top ten European heatwaves since 1950 and their occurrence in the coming decades. *Environ Res Lett* 10:124003. <https://doi.org/10.1088/1748-9326/10/12/124003>
78. Yu Z, Li Y, Wang G et al (2016) Effectiveness of elevated CO₂ mediating bacterial communities in the soybean rhizosphere depends on genotypes. *Agric Ecosyst Environ* 231:229–232. <https://doi.org/10.1016/j.agee.2016.06.043>
79. Montealegre CM, Van Kessel C, Blumenthal JM et al (2000) Elevated atmospheric CO₂ alters microbial population structure in a pasture ecosystem. *Glob Chang Biol* 6:475–482. <https://doi.org/10.1046/j.1365-2486.2000.00326.x>
80. Lee SH, Kang H (2016) Elevated CO₂ causes a change in microbial communities of rhizosphere and bulk soil of salt marsh system. *Appl Soil Ecol* 108:307–314. <https://doi.org/10.1016/j.apsoil.2016.09.009>
81. Song N, Zhang X, Wang F et al (2012) Elevated CO₂ increases Cs uptake and alters microbial communities and biomass in the rhizosphere of *Phytolacca americana* Linn (pokeweed) and *Amaranthus cruentus* L. (purple amaranth) grown on soils spiked with various levels of Cs. *J Environ Radioact* 112:29–37. <https://doi.org/10.1016/j.jenvrad.2012.03.002>
82. Cheng L, Booker FL, Burkey KO et al (2011) Soil microbial responses to elevated CO₂ and O₃ in a nitrogen-aggrading agroecosystem. *PLoS ONE* 6:e21377. <https://doi.org/10.1371/journal.pone.0021377>
83. King JS, Hanson PJ, Bernhardt ES et al (2004) A multiyear synthesis of soil respiration responses to elevated atmospheric CO₂ from four forest FACE experiments. *Glob Chang Biol* 10:1027–1042. <https://doi.org/10.1111/j.1365-2486.2004.00789.x>
84. Blagodatskaya E, Blagodatsky S, Dorodnikov M, Kuzyakov Y (2010) Elevated atmospheric CO₂ increases microbial growth rates in soil: results of three CO₂ enrichment experiments. *Glob Chang Biol* 16:836–848. <https://doi.org/10.1111/j.1365-2486.2009.02006.x>
85. Guo H, Hong C, Zheng B et al (2018) Biotechnology for biofuels improving enzymatic digestibility of wheat straw pretreated by a cellulase - free xylanase - secreting *Pseudomonas boreopolis* G22 with simultaneous production of bioflocculants. *Biotechnol Biofuels* 11:1–10. <https://doi.org/10.1186/s13068-018-1255-0>
86. Maki ML, Idrees A, Tin Leung K, Qin W (2012) Newly isolated and characterized bacteria with great application potential for decomposition of lignocellulosic. *J Mol Microbiol Biotechnol* 22:156–166. <https://doi.org/10.1159/000341107>
87. Trujillo-Cabrera Y, Ponce-Mendoza A, Rivera-Orduña FN, Wang ET (2013) Diverse cellulolytic bacteria isolated from the high humus, alkaline-saline chinampa soils. 63:779–792. <https://doi.org/10.1007/s13213-012-0533-5>
88. Zahran HH (2001) Rhizobia from wild legumes: diversity, taxonomy, ecology, nitrogen fixation and biotechnology. *J Biotechnol* 91:143–153. [https://doi.org/10.1016/S0168-1656\(01\)00342-X](https://doi.org/10.1016/S0168-1656(01)00342-X)
89. Teixeira H, Rodríguez-Echeverría S (2016) Identification of symbiotic nitrogen-fixing bacteria from three African leguminous trees in Gorongosa National Park. *Syst Appl Microbiol* 39:350–358. <https://doi.org/10.1016/j.syapm.2016.05.004>
90. Masson-Boivin C, Sachs JL (2018) Symbiotic nitrogen fixation by rhizobia — the roots of a success story. *Curr Opin Plant Biol* 44:7–15. <https://doi.org/10.1016/j.pbi.2017.12.001>
91. Li Y, Wu Z, Dong X et al (2019) Variance in bacterial communities, potential bacterial carbon sequestration and nitrogen fixation between light and dark conditions under elevated CO₂ in mine tailings. *Sci Total Environ* 652:234–242. <https://doi.org/10.1016/j.scitotenv.2018.10.253>
92. Kester RA, De Boer W, Laanbroek HJ (1997) Production of NO and N₂O by pure cultures of nitrifying and denitrifying bacteria during changes in aeration. *Appl Environ Microbiol* 63:3872–3877
93. Arai H, Kodama T, Igarashi Y (1999) Effect of nitrogen oxides on expression of the *nir* and *nor* genes for denitrification in *Pseudomonas aeruginosa*. *FEMS Microbiol Lett* 170:19–24. [https://doi.org/10.1016/S0378-1097\(98\)00517-5](https://doi.org/10.1016/S0378-1097(98)00517-5)
94. Verbaendert I, Boon N, De Vos P, Heylen K (2011) Denitrification is a common feature among members of the genus *Bacillus*. *Syst Appl Microbiol* 34:385–391. <https://doi.org/10.1016/j.syapm.2011.02.003>

95. Yang XP, Wang SM, Zhang DW, Zhou LX (2011) Isolation and nitrogen removal characteristics of an aerobic heterotrophic nitrifying-denitrifying bacterium, *Bacillus subtilis* A1. *Bioresour Technol* 102:854–862. <https://doi.org/10.1016/j.biortech.2010.09.007>
96. Feng L, Jia R, Zeng Z et al (2018) Simultaneous nitrification–denitrification and microbial community profile in an oxygen-limiting intermittent aeration SBBR with biodegradable carriers. *Biodegradation* 29:473–486. <https://doi.org/10.1007/s10532-018-9845-x>
97. Kammann C, Müller C, Grünhage L, Jäger HJ (2008) Elevated CO₂ stimulates N₂O emissions in permanent grassland. *Soil Biol Biochem* 40:2194–2205. <https://doi.org/10.1016/j.soilbio.2008.04.012>
98. Moser G, Gorenflo A, Brenzinger K et al (2018) Explaining the doubling of N₂O emissions under elevated CO₂ in the Giessen FACE via in-field ¹⁵N tracing. *Glob Chang Biol* 24:3897–3910. <https://doi.org/10.1111/gcb.14136>